Journal for ImmunoTherapy of Cancer

Infectious bursal disease virus (IBDV) as a novel oncolytic virotherapy in glioblastoma

Vicent Tur-Planells,[1,2,3] Yonina Bykov,[1] Gloria Dawodu,[1] Noemi García-Romero,[4] Sara Izpura-Luis,[2,3] Leticia Pérez-Rodríguez,[5] Sergio Rius-Rocabert,[2,3] Irina Palacín-Aliana,[3] Javier Arranz-Herrero,[2,3,6] Inmaculada Márquez-Leiva,[6] Alvaro Monago-Sanchez,[4] Maria-Luisa del Rio,[7] Jose-Ignacio Rodriguez-Barbosa ,[7] Jordi Cano-Ochando,[5,6] Adolfo García-Sastre,[1,8,9,10,11,12] Daniel Lozano-Ojalvo,[13] Estanislao Nistal-Villan ,[2,3] Angel Ayuso-Sacido,[4,14,15] Sara Cuadrado-Castano [1,10,12,16]

To cite: Tur-Planells V, Bykov Y, Dawodu G, *et al*. Infectious bursal disease virus (IBDV) as a novel oncolytic virotherapy in glioblastoma. *Journal for ImmunoTherapy of Cancer* 2025;**13**:e011741. doi:10.1136/jitc-2025-011741

► Additional supplemental material is published online only. To view, please visit the journal online (https://doi.org/10.1136/jitc-2025-011741).

Accepted 13 October 2025

For numbered affiliations see end of article.

Correspondence to
Dr Sara Cuadrado-Castano; sara.cuadrado@mssm.edu

Dr Estanislao Nistal-Villan; estanislao.nistalvillan@ceu.es

Dr Angel Ayuso-Sacido; ayusosa@vithas.es

ABSTRACT

Background Glioblastoma (GBM) is the most aggressive form of cancer of the central nervous system. Despite advances in immunotherapies and standard-of-care treatments for GBMs, clinical outcomes remain limited—owing to the immunosuppressive tumor microenvironment and the intrinsic resistance of GBM to conventional approaches. As a result, there is growing interest in rational combination strategies, particularly those pairing oncolytic viruses with immune-based therapies or established treatment modalities. Oncolytic viruses, by displaying conditionally enabled tumor cell-restricted replication, while stimulating antitumor immune responses and leaving healthy tissue unharmed, have the potential to reshape the therapeutic landscape in GBM and aid in achieving more durable benefits for patients. This study investigates the use of infectious bursal disease virus (IBDV) as a potential virotherapy for GBM.

Methods and results In vitro, IBDV infects and replicates within murine GBM cells and patient-derived GBM stem cells, inducing direct oncolysis and activating proinflammatory gene expression programs. IBDV also enhances the cytolytic activity of temozolomide (TMZ) in treated GBM cells, complementing TMZ chemotherapeutic activity. In vivo, treatment with IBDV in CT-2A GBM-bearing syngeneic mice significantly reduced tumor growth and improved survival compared with control mice. Intratumoral administration of IBDV induces a deep remodeling of the tumor immune microenvironment, reducing immunosuppressive M2-like macrophages and increasing the ratio of CD8+T cells to regulatory T cells. This reversion of immunosuppression linked to monocyte-derived macrophages has been confirmed on experimental ex vivo infections of explants derived from human GBM donors.

Conclusion These findings support further consideration of IBDV as a novel virotherapeutic agent for GBM.

WHAT IS ALREADY KNOWN ON THIS TOPIC

⇒ Glioblastoma (GBM) is the most aggressive primary brain tumor, with limited treatment options and a median survival of only 15 months despite standard care with surgery, radiotherapy, and temozolomide (TMZ). Resistance to TMZ and the immunosuppressive tumor microenvironment (TME) present significant challenges to current treatments. Oncolytic viruses (OVs) have shown promise as a therapeutic strategy by selectively infecting tumor cells and activating potent immune responses.

WHAT THIS STUDY ADDS

⇒ This study introduces infectious bursal disease virus (IBDV) as a novel oncolytic virotherapy for GBM. IBDV effectively infects and replicates in patient-derived glioblastoma stem cells and murine GBM cells, inducing tumor cell death and immune activation. The virus synergizes with TMZ to enhance cytotoxic effects and remodels the TME by reducing immunosuppressive cells, such as M2-like macrophages and regulatory T cells, while increasing cytotoxic CD8+T cells. These findings establish IBDV as a safe and potent virotherapy candidate.

HOW THIS STUDY MIGHT AFFECT RESEARCH, PRACTICE OR POLICY

⇒ IBDV's ability to complement TMZ, reduce immunosuppression, and activate antitumor immunity positions it as a promising addition to GBM treatment regimens. Its non-human origin and that avoids pre-existing immunity issues seen with other OVs in the general population. This study lays the groundwork for further preclinical and clinical research on IBDV, potentially leading to innovative combination therapies that improve patient with GBM outcomes and inform policies on oncolytic virotherapy integration into standard cancer care.

INTRODUCTION

Glioblastoma (GBM) is a diffuse astrocytic-oligodendroglial tumor. It is the most aggressive malignant primary brain tumor, which accounts for 77%–81% of all primary malignant central nervous system (CNS) tumors.[1] It is classified as a Grade 4 glioma in the latest version of the WHO (CNS5), based on molecular and histopathological features.[2] GBM is characterized by cytologically malignant, highly mitotic, and necrosis-prone neoplasms, typically associated with a high proliferation rate and rapid disease progression both before and after surgery, leading to a fatal outcome. Current treatment consists of a combination of surgery, radiotherapy, and chemotherapy with the DNA alkylating agent temozolomide (TMZ). However, despite advances in clinical diagnosis and the development of novel therapies, no effective treatment exists, and the overall survival remains at 15 months.[3] Several factors contribute to the failure of current treatments, including TMZ resistance pathways,[4] high invasive and infiltrative potential, significant intratumoral and intertumoral heterogeneity, limited access to chemotherapeutic drugs like TMZ to the CNS due to the presence of the blood-brain barrier, low permeability of blood vessels within the tumor mass,[5] a highly immunosuppressive tumor microenvironment (TME),[6] and the presence of a tumor cell subpopulation called cancer stem cells (CSCs).[7]

The study of CSCs has gained relevance due to their stem cell-like properties and their implications in tumor development and cancer prognosis. CSCs are responsible for GBM tumor dissemination through brain parenchyma,[8] contributing to glioma genesis, as well as drug resistance, metastasis, and tumor recurrence.[9] Additionally, various mutations have been identified in these tumors. Particularly interesting are the heterozygous or homozygous deletions at Ch9p21.[10] These deletions involve the genetic loss of the cyclin-dependent kinase inhibitor 2A gene (CDKN2A).[11] The type I interferon (IFN) gene cluster is in the same chromosomal region as CDKN2A, and co-deletion of both, CDKN2A and the type I IFN cluster, is common.[12 13] IFN activity functions as one of the primary immune defense mechanisms against viral infections. The absence of IFN type I cluster may render these tumors more permissive to viral replication and potentially to oncolytic therapies.[14] Therefore, it is crucial to develop new therapeutic approaches that address both the limited access to the CNS and the genetic characteristics of the tumors.

Oncolytic viruses (OVs) represent a novel class of multimechanistic therapeutic agents for cancer treatment. OVs display conditionally enabled, tumor cell-restricted replication while stimulating antitumor immune responses and leaving healthy tissue unharmed.[15] The susceptibility of cancer cells to support viral replication depends on unique molecular features mainly related to dysfunction in antiviral signaling pathways, while OVs remain inactive or unable to replicate in normal, healthy cells—where the antiviral defense machinery remains intact.[16 17] The death of tumor cells leads to the release of tumor antigens, cytokines and chemokines that stimulate the recruitment and activation of innate cells, leading to a deep remodeling of the immunosuppressive TME; importantly, the recruitment and activation of antigen-presenting cells (APCs) capable of presenting both tumor and viral epitopes is critical to achieve T cell-specific tumor elimination.[18] Numerous preclinical and early-phase clinical studies (phase I and II) have explored both DNA and RNA OVs.[19] A recent example is the conditional approval of an attenuated type I herpes simplex virus (Delytact) in Japan to treat GBM.[20] As of today, the major challenges facing OVs in GBM treatment are linked to the highly immunosuppressive microenvironment of GBM often limits viral infection, spread, and the induction of robust antitumor immune responses, as well as pre-existing antiviral immunity that can lead to rapid immune clearance of the virus and reduce treatment efficacy.[21 22]

Infectious bursal disease virus (IBDV) is a bi-segmented double-stranded RNA virus that belongs to the genus *Avibirnavirus* within the family Birnaviridae. IBDV primarily infects young domestic chickens, targeting immature IgM-bearing B lymphocytes localized in the bursa of Fabricius through several proposed surface proteins, including surface immunoglobulin M, integrin α4β1, and heat shock protein 90,[23 24] which facilitate viral attachment, internalization, and uncoating. IBDV can also infect macrophages and monocytes, although to a lesser extent.[25] As a result, chickens develop immunosuppression, making them more susceptible to opportunistic and secondary infections that can exacerbate disease severity.

To date, there have been no reports of IBDV causing infections in mammals, including humans.[26] Previous studies have explored whether IBDV can infect and replicate in mammalian cell lines—under laboratory conditions—demonstrating that IBDV typically does not establish productive infection or cytopathic effect in mammalian cells, and many IBDV strains require adaptation through serial passages to replicate efficiently in mammalian cells.[27–29] In the case of IBDV, this restriction is likely due to the incompatibility of viral entry mechanisms, the absence of the required host factors for replication, and strong mammalian antiviral defense. Yet, to date, only one report has shown IBDV ability to infect human cervix adenocarcinoma HeLa cells.[30]

In this work, we investigate the potential of IBDV as OV. As of today, several avian viruses are under investigation for cancer therapy, including Newcastle disease virus (APMV-1, Avian avulavirus 1, aka Avian paramyxovirus 1),[31 32] avian reoviruses,[33] avian avulavirus (APMV-4)[34] and certain avian influenza strains.[35] Research into avian viruses as cancer therapeutics is robust and expanding, as their inherent oncolytic features, combined with host restrictions and lack of pre-existing immunity in humans, are major advantages to be used as therapeutics in human cancer. Furthermore, IBDV has also been investigated for its potential broad-spectrum antiviral effects

in non-oncologic contexts, including the post-infection treatment of acute and chronic viral diseases, reinforcing its safety and therapeutic versatility beyond cancer.[36]

Here, we have studied responses elicited by IBDV in different models of GBM. In addition to inducing tumor cell oncolysis, IBDV stimulates antiviral and proinflammatory immune responses in different glioma cells. In vitro, the susceptibility of GBM cells to IBDV infection and killing is further boosted in combination with the chemotherapeutic TMZ—current standard of care in GBM management. In preclinical studies in mice, intratumoral administration of IBDV delays tumor growth, concomitant to a robust immune cell remodeling at the TME. In human explant studies, short exposure to IBDV demonstrates a reduction of the immunosuppressive nature of GBM TME.

MATERIAL AND METHODS

Cell lines and viruses

Murine glioma cell lines CT-2A (ATCC cat# SCC194) and GL261 (ATCC cat# ACC 802) were maintained in Dulbecco's Modified Eagle Medium (DMEM)/F-12 supplemented with 10% FBS (Fetal Bovine Serum), 1% antibiotics, and 2 mM of L-glutamine. Human patient-derived primary GBM cells (GBM18 and GBM27) were obtained according to García-Romero, González-Tejedo *et al*, and subcultured in supplemented DMEM/F-12 (Gibco, 11039) containing non-essential amino acids (10 mM; Gibco, 11140), Hepes (1 M; Gibco, 15630), D-glucose (45%; Sigma, St. Louis, Missouri, USA; G8769), BSA-F5 (7.5%; Gibco, 15260), sodium pyruvate (100 mM; Gibco, 11360), L-glutamine (200 mM; Gibco, 25030), antibiotic-antimycotic (100×; Gibco, 15240), N2 supplement (100×; Gibco, 17502), hydrocortisone (1 µg/µL; Sigma, H0135), tri-iodothyronine (100 µg/mL; Sigma, T5516), EGF (25 ng/µL; Sigma, E9644), bFGF (25 ng/µL; Sigma, F0291), and heparin (1 µg/µL; Sigma, H3393). QM7 cells (ATCC cat# CRL-1962) were cultured in DMEM supplemented with 10% FBS. Murine BMDMs (Bone Marrow-Derived Macrophages) were isolated from the femur, tibia, and fibula of bone marrow of 8-week-old C57BL/6 mice. Bone marrow was liberated through the injection of phosphate-buffered saline (PBS) and clogs were disaggregated mechanically by a syringe. Afterwards, cells were centrifuged for 5 min at 1,500 rpm and the supernatant was discarded. Finally, cells were resuspended in RPMI (Roswell Park Memorial Institute medium) medium supplemented with GM-CSF (Granulocyte-Macrophage Colony-Stimulating Factor) (Gibco, Waltham, Massachusetts, USA) (30 ng/mL) before plating. After 4 days, cell medium was replaced with a fresh stock for 3 more days to complete cell differentiation before viral infections. The human microglia HMC3 cell line (ATCC cat# CRL-3304) was maintained in DMEM supplemented with 10% FBS. Cells were maintained at 37°C with 5% of CO_2 and 90% humidity.

IBDV, Soroa strain, and serotype I, being low pathogenic in birds, were provided by Professor José F Rodríguez (CNB-CSIC, Spain); viral stocks were propagated in QM7 cells and cleared-purified following the protocol previously described.[37] The recombinant Newcastle disease virus LaSota strain NDV-LS-L289A, was propagated in 9-day-old chicken-embryonated eggs and clear-purified by ultracentrifugation in 30% sucrose gradient.

Fluorescence microscopy and image acquisition

Cancer cells were infected at the indicated multiplicity of infection (MOI) for 24 hours. Cell fixation was performed using 2% paraformaldehyde in PBS for 10 min. Cell membrane permeabilization was carried out using 0.2% Triton-PBS for 10 min and blocked in PBS 1% BSA (Bovine Serum Albumin) for 1 hour. Specific antibodies used for indirect immune detection are described in online supplemental table 1. Images were taken using an EVOS FL cell imaging system (Thermo Fisher Scientific).

Virus replication kinetics and tittering assays

Supernatants of IBDV-infected GBM cells at corresponding time points were tittered

in QM7 cells plated the day before in 96-well plates in DMEM supplemented medium. IBDV supernatants were diluted by 1/10 dilutions in DMEM supplemented medium and left on QM7 cells for 72 hours. Negative control wells had GBM supernatants without IBDV infection. The cytopathic effect was analyzed by optical microscopy 72 hours post-infection. Tissue culture infectious dose 50 (TCID50/mL) viral titers were calculated using the Reed-Muench method.[38]

Viability assays

An (3-(4,5-dimethylthiazol-2-yl)-5-(3-carboxymethoxyphenyl)-2-(4-sulfophenyl)-2H-tetrazolium) MTS assay was used to assess cell viability. A total of 1×10^4 cells per well were plated in a 96-well plate containing complete medium and allowed to adhere for 24 hours. After attachment, cells were treated with TMZ or infected with IBDV or NDV-LS viruses for the corresponding experimental conditions. PBS was used as a control, with five replicate wells per condition. After the designated treatment time, 20 µL of MTS solution (5 mg/mL) was added to each well. The plates were then incubated at 37°C, protected from light, for 1.5 hours. Following incubation, the solutions in the wells were mixed, and absorbance was measured at 450 nm (for tetrazolium salts) and 630 nm (for background) using a microplate reader (Varioskan Lux). Relative cell viability was calculated as the percentage of absorbance compared with the control group.

Western blots

Protein was extracted from the cultured cells with radioimmunoprecipitation lysis buffer on ice and centrifuged at 12,000×g for 15 min at 4°C to eliminate cell debris. The total protein concentration was determined using a Bicinchoninic Acid (BCA) protein assay kit, and whole lysates mixed with 5×sodium dodecyl sulfate (SDS)

loading buffer were denatured with a 5 min incubation at 95°C. Then, equal amounts of protein were separated by SDS-polyacrylamide gel electrophoresis and transferred to a polyvinylidene difluoride membrane. Blocked membranes were then incubated with their corresponding antibodies described in online supplemental table 1. The horseradish peroxidase immune complexes were detected using an enhanced chemiluminescence kit (Alkali Scientific) in a ChemiDoc imaging system (Bio-Rad).

Transcription analysis by qRT-PCR

Cells were mock treated or infected with the specified virus at an MOI of 3 Plack formation units (PFU)/cell in 500 µL of OptiMEM-I. After allowing virus adsorption for 1 hour, the cells were incubated with an additional 1,500 µL of supplemented media. Total RNA was isolated using a Qiagen RNeasy Minikit (catalog no.74106, Qiagen) at the indicated time post-infection. Complementary DNA (cDNA) synthesis was performed using the Maxima First Strand cDNA Synthesis Kit for quantitative Real-time reverse transcription-polymerase chain reaction (RT-PCR) (catalog no. K1671, Thermo Fisher Scientific). Mean n-fold expression levels of cDNA from three individual biological samples were normalized to housekeeping gene levels and calibrated to mock-treated samples according to the $2^{-\Delta\Delta Ct}$ method.[39] Results are expressed as relative cycle threshold (Ct) values to the mock-treated group. Human and murine primer sequences are compiled in online supplemental table 2.

Histological staining

Spleen, bone marrow, lymph nodes, and liver were harvested in 9-week-old C57BL/6 mice after 24 hours of one IBDV (10^7 PFU) tail vein injection for systemic administration (n=3). PBS was used for negative controls. Tissue fragments were fixed in a 4% buffered formalin solution, pH 7.2, for 24 hours. The buffer was changed to ethanol solution 70% and organs were embedded in paraffin. Paraffin blocks of each organ were cut in a microtome (3 µm slices) and mounted on slides prior to routine histological analysis (H&E). Histological slides were qualitatively analyzed under light microscopy.

Systemic and intracranial virus delivery studies

9-week-old C57BL/6 mice (Charles River Laboratories, Wilmington, Massachusetts, USA) were stereotactically injected with viral doses of 10^4, 10^5, and 10^6 PFU into the striatum of the right hemisphere (0 mm anterior and 2.5 mm lateral to the bregma; 3.5 mm intraparenchymal). PBS was used as a control vehicle. Mice weight was monitored weekly for 6 weeks. Procedures used on mice were approved by and performed according to the guidelines of the institutional animal-care committee of Universidad Francisco Vitoria under the accession PROEX 142.8/24.

The protocol for biodistribution studies was approved by Universidad de Leon under the access OEBA-ULE-001–2023.

Tumor model

Tumor progression and survival studies were performed following Institutional Animal Care and Use Committee (IACUC) guidelines and have been approved by the IACUC of Icahn School of Medicine at Mount Sinai (IACUC-2014–0234). 6–8 weeks old of age female C57BL/6J mice used in our in vivo studies were purchased from Jackson Laboratory.

1.5×10^6 CT-2A cells were intradermally engrafted on the right hind leg and tumors were allowed to grow to 50 mm^3 before treatment initiation. Tumor-bearing mice were treated by intratumoral injection of IBDV, NDV, or PBS with viral doses of 1×10^7 PFU/50 µL PBS. Intratumoral injections were administered every other day for a total of four treatment doses or as specified for downstream analysis or tissue samples. Tumor volume was monitored every 48 hours, and every 24 hours as tumor volumes approached the experimental endpoint of 1,000 mm^3. Mice were humanely euthanized on the day when the volume exceeded the predefined endpoint or at any sign of distress, including tumor ulceration. Tumor measurement was determined using a digital caliper, and the total volume was calculated using the formula: tumor volume (V)=L2×W, where L (tumor length) is the larger diameter and W (tumor width) is the smallest diameter.

Human GBM explants study

Human GBM-isocitrate dehydrogenase (IDH) wild-type tumor biopsy was obtained from the Biobank of Hospital Universitario Puerta de Hierro Majadahonda/Instituto de Investigación Sanitaria Puerta de Hierro-Segovia de Arana. Ethical approval for the use of these samples was granted by the institutional review board of HM Hospitals (CEIm No: 23.06.2206-GHM). All patients provided written informed consent prior to enrollment, and all procedures were conducted in accordance with the principles of the Declaration of Helsinki. Fresh tumor samples were placed in ice-cold Hibernate-A medium supplemented with penicillin-streptomycin immediately after resection and processed within 2 hours of surgery. GBM tissue was cut into 20–30 mm^3 fragments under a dissection microscope, washed three times with ice-cold PBS, and then placed in 24-well plates containing specialized growth medium (DMEM-F12, Neurobasal, non-essential amino acids, N2 supplement, B27 supplement, human insulin, penicillin-streptomycin, and 2-mercaptoethanol). The tissue slices were maintained at 37°C in a humidified atmosphere with 5% CO_2. Explants were subjected to TMZ treatment (1 mM) and/or IBDV infection (10^7 PFU) and cultured for 72 hours prior to downstream processing and flow cytometry analysis.

Flow cytometry

Murine tumors and tumor-draining lymph nodes (tdLN) were excised from terminated animals at the indicated time points and tissues were processed for downstream analysis by flow cytometry. Briefly, samples were incubated in FC-blocking antibody

(BD #553141) diluted in Fluorescence-Activated Cell Sorting FACS buffer (1% BSA, 0.5 mM EDTA in PBS) for 20 min on ice, then resuspended in Fixable Viability Dye eFluor 780 (Thermo Fisher #65-0865-14; 1:3000) in PBS for 10 min at room temperature. Samples were incubated with corresponding extracellular antibodies prepared in FACS buffer for 30 min. Samples were then fixed according to manufacturer's instructions using the eBioscience Foxp3/Transcription Factor Staining Buffer Set (Thermo Fisher, Ref. 00-5523-00). Intracellular staining was performed in permeabilization wash buffer (eBioscience, Ref. 00-8333–56/88-8824-00). Antibodies used for intracellular and extracellular staining of isolated immune cells are itemized in (online supplemental table 1). Samples were run on an LSRFortessa X-20 flow cytometer (BD); immunophenotyping analysis was performed using FlowJo V.10 software.

Single-cell isolation from GBM explants for spectral flow cytometry analysis

GBM tumor biopsy specimens were preserved in MACS Tissue Storage Solution (Miltenyi Biotec, Bergisch Gladbach, Germany), maintained at 48°C, and processed within 3 hours after collection. To obtain single-cell suspensions, samples were enzymatically digested in 10 mL of RPMI with Ca2+/Mg2 +(Gibco) containing 2% FBS (ATCC, Manassas, Virginia, USA), 0.5 mg/mL DNase I (grade II, from bovine pancreas; Roche, Penzberg, Germany), and 0.5 mg/mL collagenase IV (Gibco) for 40 min at 37°C with continuous shaking of 150 rpm. Tissues were disrupted, passed through a 70 mm cell strainer, and washed two times with RPMI medium (Gibco). Isolated cells were centrifuged and directly used for phenotyping. Immune phenotyping of GBM biopsy specimens was performed by staining the cells for spectral flow cytometry analyses using the flow antibodies listed in online supplemental materials, and samples were acquired with a Cytek Aurora 5-laser cytometer (Cytek Biosciences, Fremont, California, USA). Immunophenotyping analysis was performed using FlowJo V.10 software.

Statistical analysis

Data analysis was performed using GraphPad Prism V.10 package. One-way analysis of variance (ANOVA) or two-way ANOVA was used to compare multiple groups with one or two independent variables, respectively. Results are expressed as mean value±SEM or ±SD as indicated. Comparisons of survival curves were performed using the log-rank (Mantel-Cox) test. Survival analysis was carried out using the Kaplan-Meier method. P values>0.05 were considered statistically non-significant; *p<0.05; **p<0.01; ***p<0.001; ****p<0.0001.

RESULTS

Patient-derived GSCs and murine GBM models support IBDV replication

While the cell cycle and immune responses to IBDV have been vastly covered in chicken models, our current understanding of the capacity of IBDV to infect and drive antiviral responses in mammalian cancer cells is limited to a single study performed using HeLa cells.[40]

To assess the ability of IBDV to infect brain cancer cells, murine gliomas (CT-2A, GL261) and patient-derived glioblastoma stem cells (GSCs), monolayers were exposed to IBDV for 24 hours. Indirect immunodetection targeting the viral protein VP3 revealed that IBDV is capable of efficiently infecting both human and murine cancer cells (figure 1A). Furthermore, all tested cancer cell types supported productive viral replication, as demonstrated by the cumulative recovery of infectious viral particles over the course of 120 hours (figure 1B,C). Additionally, IBDV displayed differences in replication kinetics and viral titers in a cell-specific manner: in murine GBMs, earlier accumulation of VP3 protein in GL261 cells (online supplemental figure S1) correlated with an increase in viral titers over time when compared with CT-2A cells (figure 1B). In the case of human GSCs (figure 1C), there was a strong correlation between the capability of the infected cells to induce type-I IFN responses during viral infection and limit IBDV production (GBM18), as compared with GBM 27, which lacked the type I IFN cluster[14] and rendered a higher viral yield. These data present evidence of the distinct cell-dependent behavior of IBDV in different mammalian brain cancer cells.

Additionally, the cytopathic effect of IBDV infection was evaluated in different GBM cells, including the GSCs GBM18 and GBM27. Microscopy analysis at 120 hours post-inoculation revealed a direct correlation between higher MOIs and an increased cytopathic effect, noticed by the presence of cellular debris and small vesicles (figure 1D,E). Remarkably, IBDV effectively disrupted GBM27 sphere architecture at an MOI as low as 1.

MTS assay was used to evaluate the impact of the infection on cell viability at 24, 48, and 72 hours post-infection (hpi) with cells now exposed to a fixed MOI of 3 (figure 1F–I). The kinetics of the cytopathic effect of IBDV were compared with those of the NDV-LS as a reference.[41] The results showed that IBDV significantly reduced the viability of human and murine GBM cells at 72 hpi compared with NDV-LS in murine CT2A and GL261. In CT-2A and GL261 cells, a rebound effect was observed, where the cell viability increased at this time point, allowing for resumed growth and counteracting the effects of NDV-LS infection (figure 1F,G). In GBM 18 and GBM 27 cells, both viruses reach their peak cytotoxic effect at 72 hpi, with similar kinetics (figure 1H,I). In contrast, experimental infection of HFF-1 human fibroblast cell line cells showed no detectable viral replication at 72 hpi, with titers remaining low (10^1–10^2 $TCID_{50}$/mL), as shown in online supplemental figure S2B. Viability assays conducted at 48 and 72 hpi—time points when

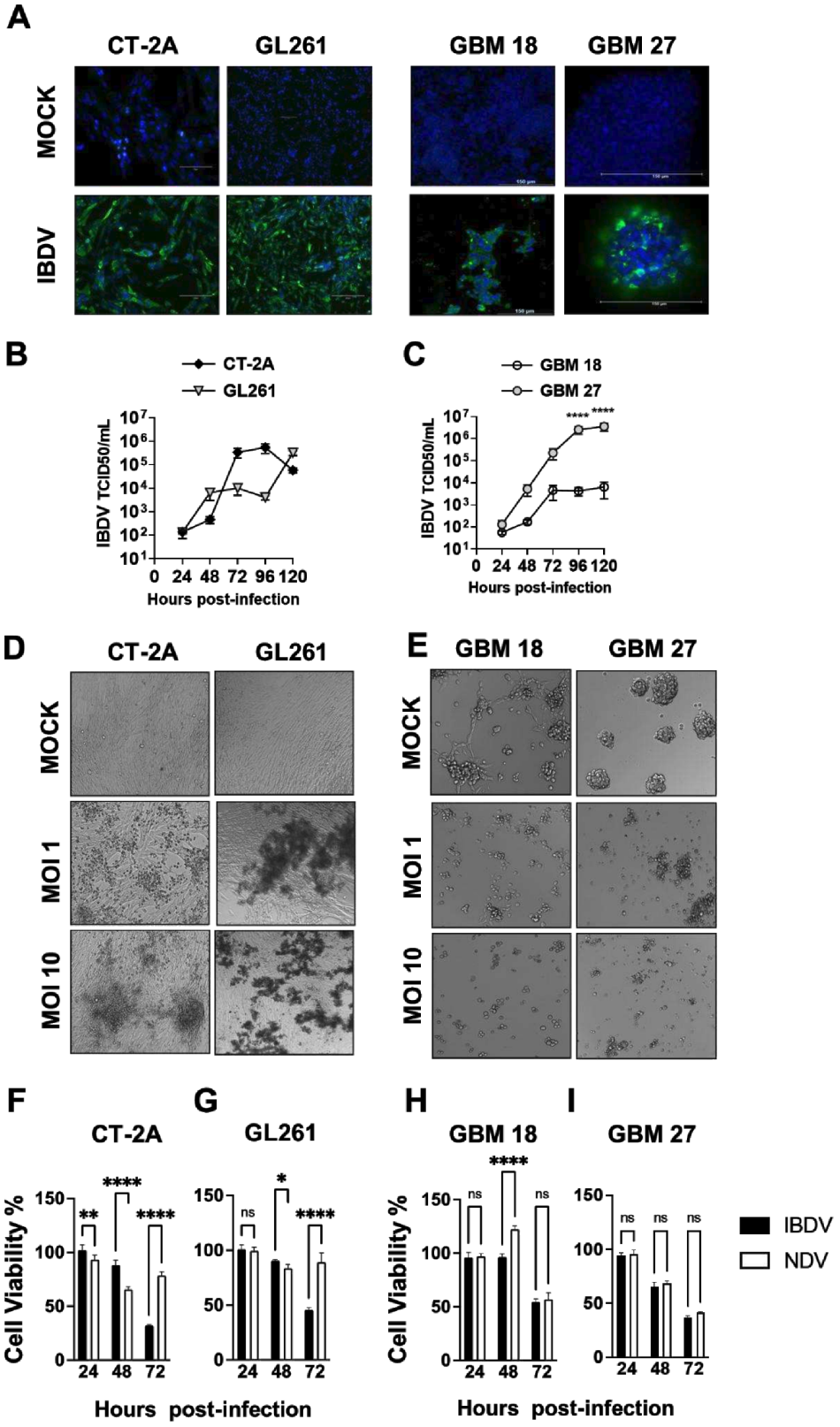

Figure 1 Infectivity and replication capacity of IBDV in murine GBM and patient-derived GSC cells. (A) Indirect Immunofluorescence microscopy: immunodetection of IBDV's VP3 protein on GBMs 24 hours post viral exposure (MOI=3). Images were taken at 40× magnification. (B, C) IBDV's replication kinetics—growth curves: viral titers were calculated by TCID50/mL method; initial input=MOI 0.01 (n=3). (D, E) Cytopathic effect: brightfield microscopy of GBMs monolayers 120 hours post-infection with IBDV at specified MOI. 20× magnification. (F, G, H, I) Viability analysis: cell viability was assessed via standard MTS assay at indicated times post infection (24, 48, and 72 hours). Two-way ANOVA analysis: *p<0.05; ***p<0.001; ****p<0.0001. ANOVA, analysis of variance; GBM, glioblastoma; GSC, glioblastoma stem cell; IBDV, infectious bursal disease virus; MOI, multiplicity of infection; ns, non-significant; TCID50, tissue culture infectious dose 50.

IBDV induces cytotoxic effects in GBM cells—showed no decrease in fibroblast viability (online supplemental figure S2C). These findings confirm IBDV's capability to effectively infect, replicate and induce oncolysis in vitro across different brain cancer cells, including patient-derived GSCs and murine GBM cell lines with minimal impact in survival on healthy cells.

IBDV infection triggers type-I interferon and pro-inflammatory cytokine release in GBMs

Viruses with therapeutic potential against diverse tumors have been demonstrated to stimulate antiviral responses in infected cells. This primarily involves the induction of type-I IFN and cytokine release and ultimately promotes the activation of cell death programs.[42 43]

To study the intrinsic immunological response of GBM cells to IBDV infection, murine and human GBMs, including the human GSCs GBM18 and 27, were infected with IBDV at an MOI=3 for 16 hours. Subsequently, we analyzed the expression of IFNs (*IFNB1, IL28*) and the IFN-stimulated gene *MX1* as well as pro-inflammatory (*IL1B*, *IL6*) by RT-qPCR. The clinical candidate NDV-LS virus was included as reference for comparative purposes. Both murine and human GBM infected cells trigger a moderate type I IFN response, characterized by the expression of *IFNB1* and *MX1* genes, together with induction of type-III IFN (*IL28B*) cytokines and pro-inflammatory genes (figure 2A–D), similarly to the effect elicited by NDV-LS infection.

During natural infection, IBDV has been shown to exert modulatory effects on cells of the monocyte-macrophage lineage (Mo-Macs), with IBDV-infected Mo-Macs releasing chemotactic, proinflammatory and immunoregulatory cytokines.[44] This delays the resolution of the viral infection and associated pathology in its natural host. In GBM, tumor-associated macrophages (TAMs) and microglia are the most abundant immune cell populations in the TME and the major drivers of immunosuppression and progression of the disease.[45] Due to their relevance in GBM biology, IBDV-triggered pro-inflammatory gene expression signatures in mammalian murine bone-marrow-derived macrophages (M1-Mo) and HCM3 human microglia myeloid-derived cells were analyzed by RT-qPCR 72 hours after exposure to the virus (figure 2E,F). IBDV stimulates *MX1* gene expression in both cell types and, consistently with the responses observed in GBMs, to a lower extent than NDV-LS, highlighting IBDV's moderate inflammatory behavior. Gene expression analysis of infected HFF-1 human fibroblast cell line revealed that it activates an antiviral response, with expression of IFN-β and Mx1 detected at 24 hpi (online supplemental figure S2D). These latest results further support the lack of antagonism of type-I IFN signaling of IBDV in healthy human cells.

Overall, these findings indicate that IBDV infection induces a moderate immunostimulatory effect across different GBM cells, including patient-derived and murine lines, as well as in mouse and human myeloid cells and that mammalian healthy cells can efficiently counteract the replication of IBDV through the activation of antiviral signaling pathways.

Combination of IBDV and TMZ exhibits synergistic impact on GBMs survival

TMZ is the standard first-line treatment for patients newly diagnosed with gliomas.[46] However, approximately 50% of GBMs exhibit resistance to TMZ, which can be attributed to both intrinsic and acquired resistance mechanisms.[4] TMZ-induced cell death presents differences in the murine and human GBM models under the current study (figure 3A–C). Specifically, the human GBM27 cell line was the most refractory to TMZ treatment, while GBM18 exhibited a dose-dependent response. In contrast, murine GBM cells (CT-2A) showed the greatest reduction in cell viability at lower TMZ doses.

Considering these phenotypes—the differential sensitivity to TMZ by GBMs, we next investigated whether TMZ treatment could alter the susceptibility of GBM cells to IBDV infection (figure 3D–F). At 0.5 mM, the viability of GBM cell lines and GSCs decreases to around 60% with TMZ administration alone, having a similar impact on cell viability as IBDV infection only. Interestingly, concomitant administration of TMZ and IBDV significantly reduced viability when compared with each treatment individually. Follow-up highest single-agent statistical analysis confirmed a synergistic effect of both treatments reducing GBM cell viability, with a remarkable impact on GBM27 cells. Data to assess the combinatory effect of both treatments is compiled in (figure 3G–I and online supplemental figure S3A). Furthermore, sustained exposure to TMZ and IBDV demonstrated a dual effect in GBMs: the reduction in cell viability exerted by the combination was accompanied by enhanced IBDV replication (online supplemental figure S3B and C), as indicated by a significant increase in viral release at the peak of replication (72 hpi). This boost in viral production was not a reflection of a diminished antiviral responses, as indicated by the levels of expression of IFN-β and MX1 genes (online supplemental figure S3D and E).

These results highlight the complementary and synergistic interaction between TMZ and IBDV in GBM models that exhibit different sensitivity to the chemotherapeutic TMZ. The clear effects demonstrated in vitro merit further investigation to clarify its mechanisms and clinical implications.

Intratumoral administration of IBDV results in control over tumor growth and extended survival in CT-2A tumor-bearing mice

Our in vitro studies demonstrated that IBDV can induce both immunostimulatory and cytotoxic responses in various GBMs, exhibiting a profile similar to that of the clinical OV candidate NDV-LS. To assess the feasibility of using IBDV as a therapeutic

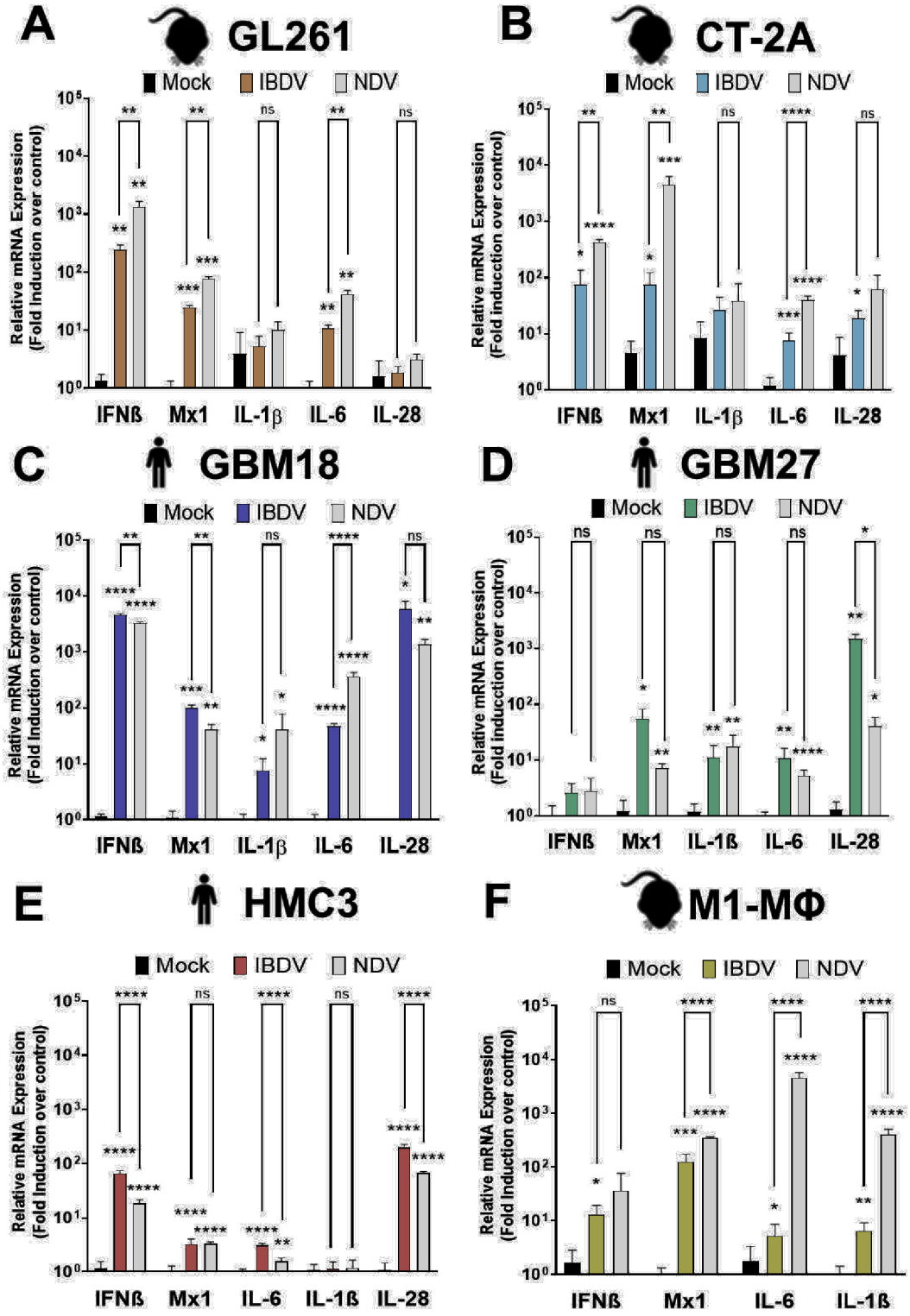

Figure 2 Antiviral and pro-inflammatory gene expression triggered by IBDV infection. Gene expression analysis (RT-qPCR). Cancer cell monolayers (A–D), bone-marrow-derived macrophages and human microglia HCM3 (E–F) cells were infected with IBDV and NDV-LS at an MOI=3 for 16 hours. Expression levels for each individual gene were calculated as log10 of fold induction over mock-infected cells. Two-way ANOVA analysis: *p<0.05; ***p<0.001; ****p<0.0001. ANOVA, analysis of variance; IBDV, infectious bursal disease virus; IFN, interferon; IL, interleukin; MOI, multiplicity of infection; mRNA, messenger RNA; ns, non-significant.

for GBM, we first conducted safety studies in immunocompetent C57Bl/J6 mice through both systemic and intracranial administration of IBDV (figure 4A,B). Histological analysis of tissue samples, 24 hours after systemic inoculation of a high dose of IBDV (10^7 PFU), revealed no virus-associated pathology in any

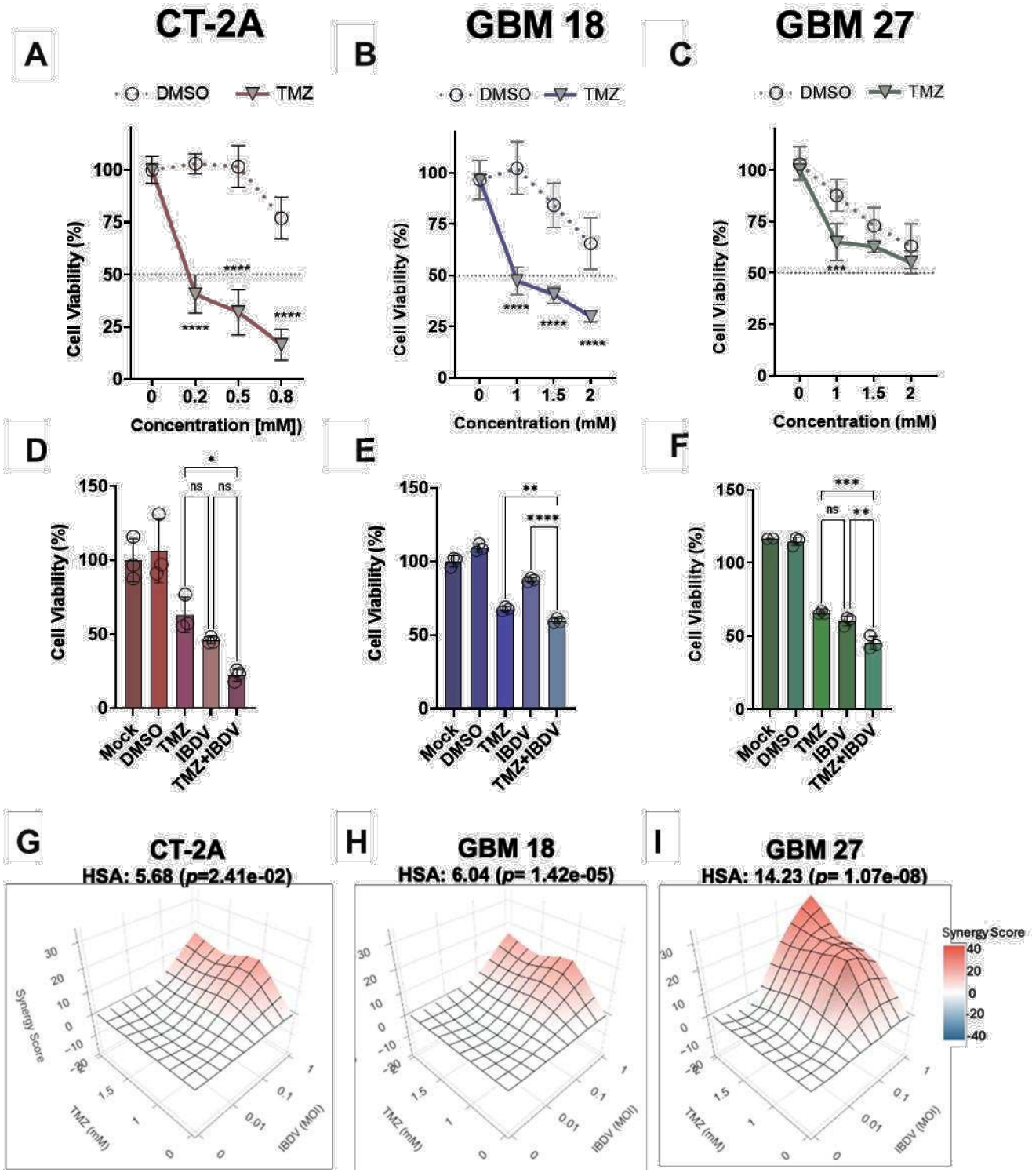

Figure 3 Combinatory effect of TMZ with IBDV. (A, B, C) TMZ cytotoxicity analysis: at 72 hours, cell viability was measured via standard MTS assay compared with a Mock control after treatment with different concentrations of TMZ (DMSO control concentrations correspond to the final concentrations of TMZ used in each condition). (D, E, F) Combination effect of TMZ and IBDV: GBM cell viability was measured after treatment with 0.5 mM of TMZ, IBDV infection (MOI 1), or both conditions together. (G, H, I) HSA statistical test: the HSA statistical analysis was performed based on the effect of drug combinations relative to the effect of each treatment alone to assess additive, synergistic or antagonistic effects. DMSO was used as the vehicle for TMZ, and final DMSO concentrations in each well correspond to those of the TMZ treatments (eg, 2 mM TMZ corresponds to 2% DMSO). Equivalent DMSO concentrations were included in vehicle controls. Two-way ANOVA analysis: *p<0.05; ***p<0.001; ****p<0.0001. ANOVA, analysis of variance; GBM, glioblastoma; HSA, highest single agent; IBDV, infectious bursal disease virus; MOI, multiplicity of infection; ns, non-significant; TMZ, temozolomide.

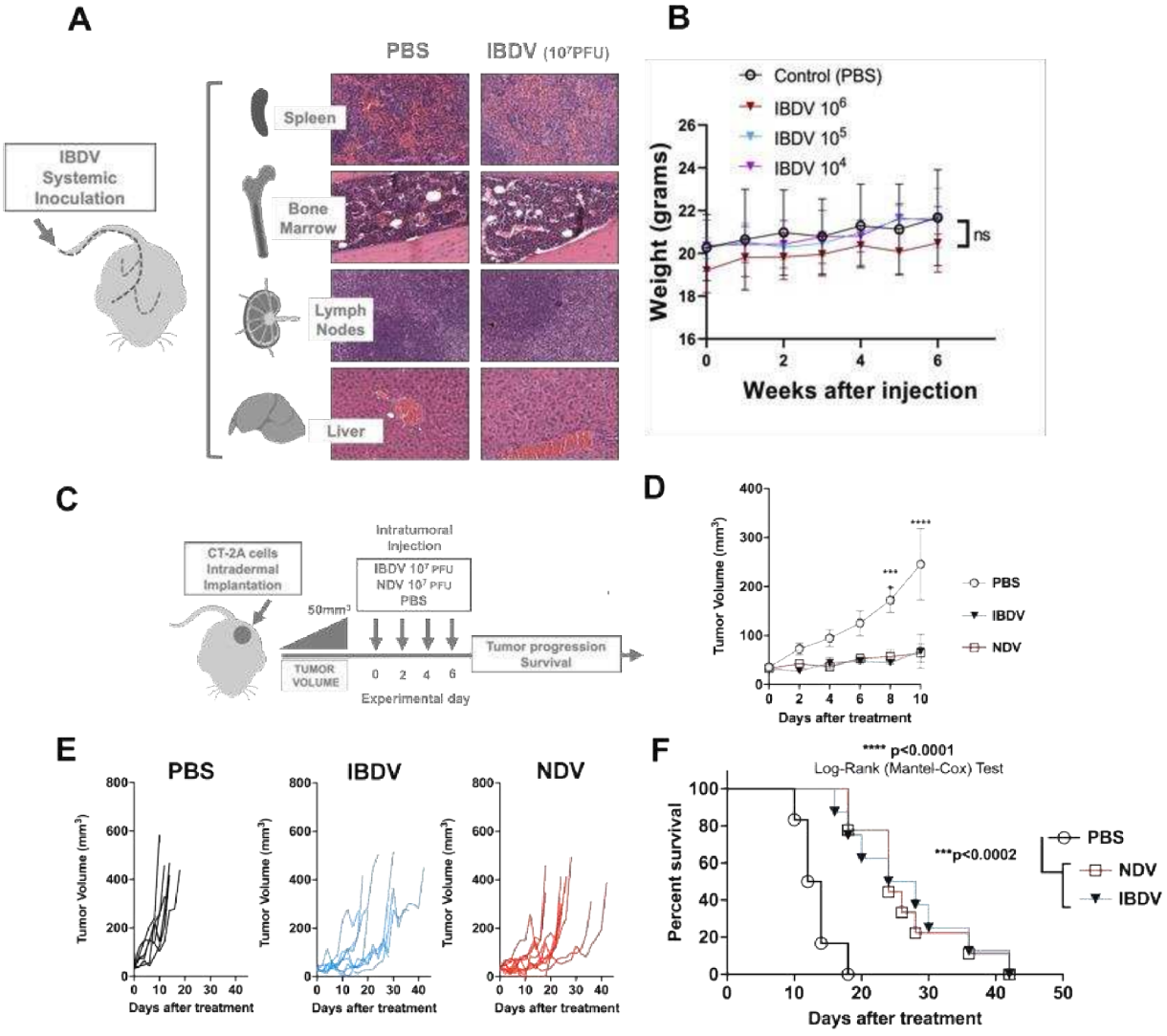

Figure 4 In vivo antitumor effect of IBDV. (A–B) Pathogenicity studies. (A) 6–8 weeks old C57BL/6 mice (N=3) were intravenously administered with either PBS or 10^7 PFU of IBDV; H&E histochemistry of indicated organs processed 24 hours post systemic viral dissemination. (B) IBDV intracranial toxicity: body-weight progression of C57BL/6 mice (N=3) after exposure to a single intracranial injection of IBDV at the indicated dose. (C–E) Antitumor capacity of IBDV. (C) Schematic representation of the study. CT-2A tumor-bearing mice were intratumorally administered 10^7 PFU of IBDV/NDV or PBS, once every other day, for a total of four doses. Tumor volume was monitored every 48 hours. Experimental end-point: 1,000 mm3 tumor volume. (D) Average of tumor volume per experimental group at the time of first death. Two-way ANOVA. *p<0.05, **p<0.01. (E) Individual tumor growth curves. (F) Survival analysis: log-rank (Mantel-Cox) test. ***p<0.001, ****p<0.0001. ANOVA, analysis of variance; IBDV, infectious bursal disease virus; PBS, phosphate-buffered saline.

organ or tissue processed. Additionally, no signs of distress were detected in any of the experimental animals. Similarly, exploratory intracranial administration of IBDV at high doses resulted in absence of morbidity or mortality over the 6-week study period (figure 4B).

Next, we investigated if IBDV could drive antitumor responses in a syngeneic CT-2A experimental tumor model developed in the flank of immunocompetent mice. As a reference and for comparative purposes, we included an experimental group treated with NDV-LS virus (figure 4C). Results showed that both IBDV and NDV-LS treatments can control tumor growth (figure 4D) compared with untreated control mice. Individual tumor growth volume curves indicated that while none of the viruses could completely inhibit tumor progression, both treatments significantly delayed tumor growth compared with PBS-treated controls (figure 4E). Moreover, both IBDV and NDV-LS treatments significantly extended survival in treated mice compared with the control group (figure 4F). No signs of distress or morbidity associated with IBDV treatment were observed in any of the experimental animals.

Overall, these results confirmed that IBDV is safe in immune-competent mice and exhibits significant oncolytic activity, comparable to NDV-LS, in delaying CT-2A GBM progression and improving mouse survival.

IBDV virotherapy remodels TME reducing immunosuppression priming tumors for cytotoxic responses

The architecture and immune landscape of the TME are critical determinants of the efficacy and durability of targeted antitumor responses.[47]

Given that IBDV demonstrated a beneficial antitumor effect in GBM in vivo, we assessed changes in immune cell populations within the TME. Mice were divided into two groups: those receiving either a single injection (Day 1) or three injections (Day 5) of IBDV (10^7 PFU), compared

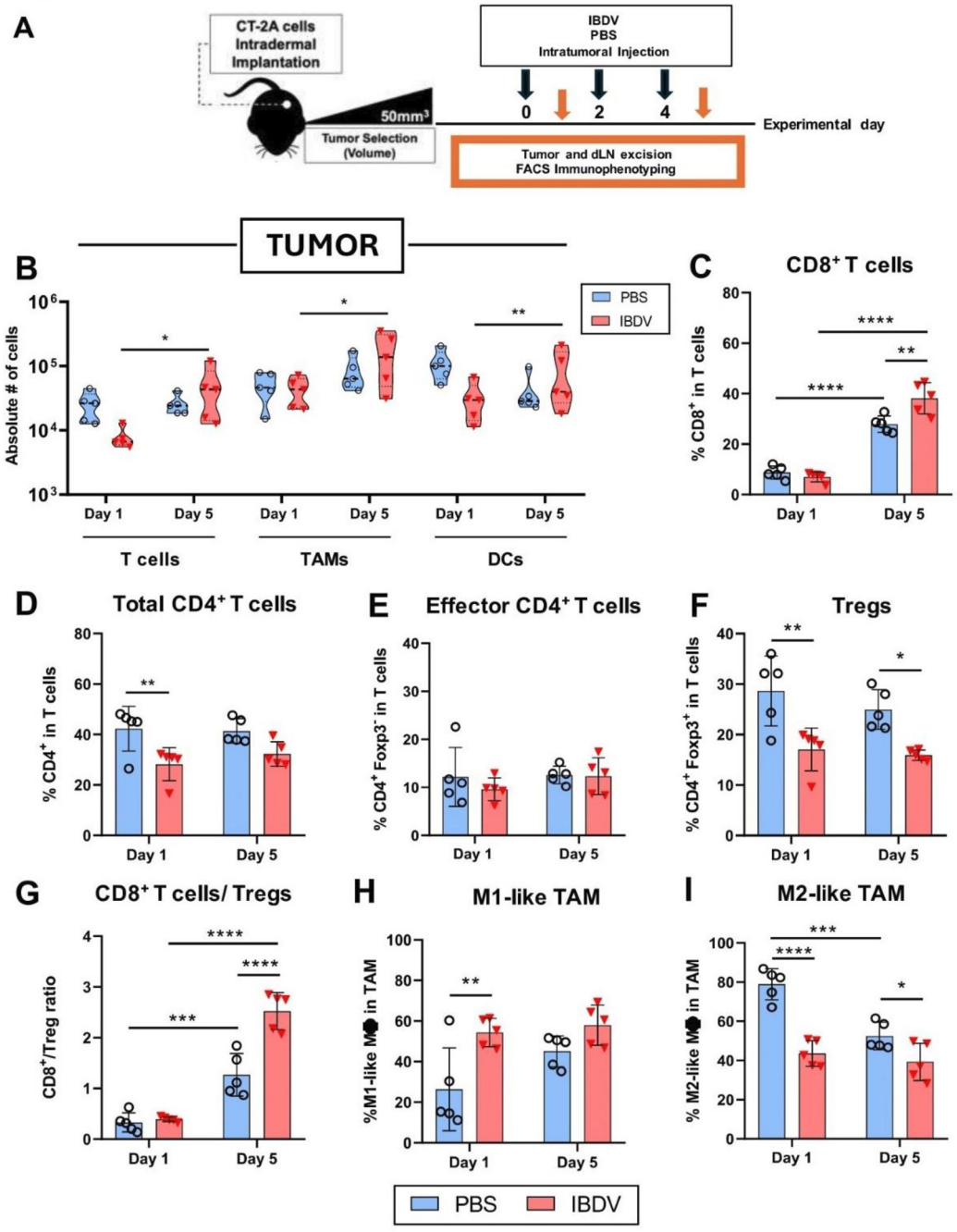

Figure 5 Immunostimulation of innate and adaptive immune response in TME on IBDV treatment in CT-2A murine GBM model. (A) Schematic representation of the study: CT-2A tumor-bearing mice were intratumorally treated every other day with a total of either one or three doses of 10^7 PFU of IBDV. Mice were sacrificed 1 day after the first or third injection in which tumor masses (TME) were harvested and probed with primary-conjugated antibodies against main biomarkers of immune cells. (B) Analysis of main immune populations in TME: temporal distribution of immune cell populations within TME of IBDV/PBS-treated mice. (C–J) Analysis of myeloid and lymphoid immune cell populations in TME: changes in innate and adaptive immune response in IBDV-treated compared with PBS-treated mice were analyzed in both groups (day 1 and 5). Two-way ANOVA analysis: *p<0.05; ***p<0.001; ****p<0.0001. ANOVA, analysis of variance; dLN, draining lymph nodes; GBM, glioblastoma; IBDV, infectious bursal disease virus; PBS, phosphate-buffered saline; TAM, tumor-associated macrophage; TME, tumor microenvironment; Treg, regulatory T cell.

with PBS-treated controls (figure 5A), to identify earlier (Day 1) and delayed (Day 5) immunological changes in the tumor composition induced by IBDV treatment. Flow cytometry was employed to analyze lymphoid and myeloid immune cell populations, using the gating strategy outlined in online supplemental figure S4.

Analysis of treated tumors revealed differential enrichment of T cells, macrophages, and Dendritic cells (DCs) in IBDV-treated tumors when compared with control mice (figure 5B). Specifically, mice receiving three doses of IBDV exhibited an enrichment in CD8+T (figure 5C), while those treated with a single injection showed a decrease in total CD4+T cells (figure 5D) compared with controls. This reduction in total CD4+T cells was associated with a decrease in immunosuppressive regulatory T cells (Treg) (figure 5F), rather than effector T cells (figure 5E). These findings suggest that IBDV breaks TME immunotolerance, facilitating cytotoxic T-cell functions, as defined by a higher CD8+T cell/Treg ratio after repeated doses of IBDV (figure 5G).

Analysis of the myeloid compartment showed a reduction in the presence of immunosuppressive M2-like macrophages (CD11c−, CD11b+, Ly6G−, Ly6C−,

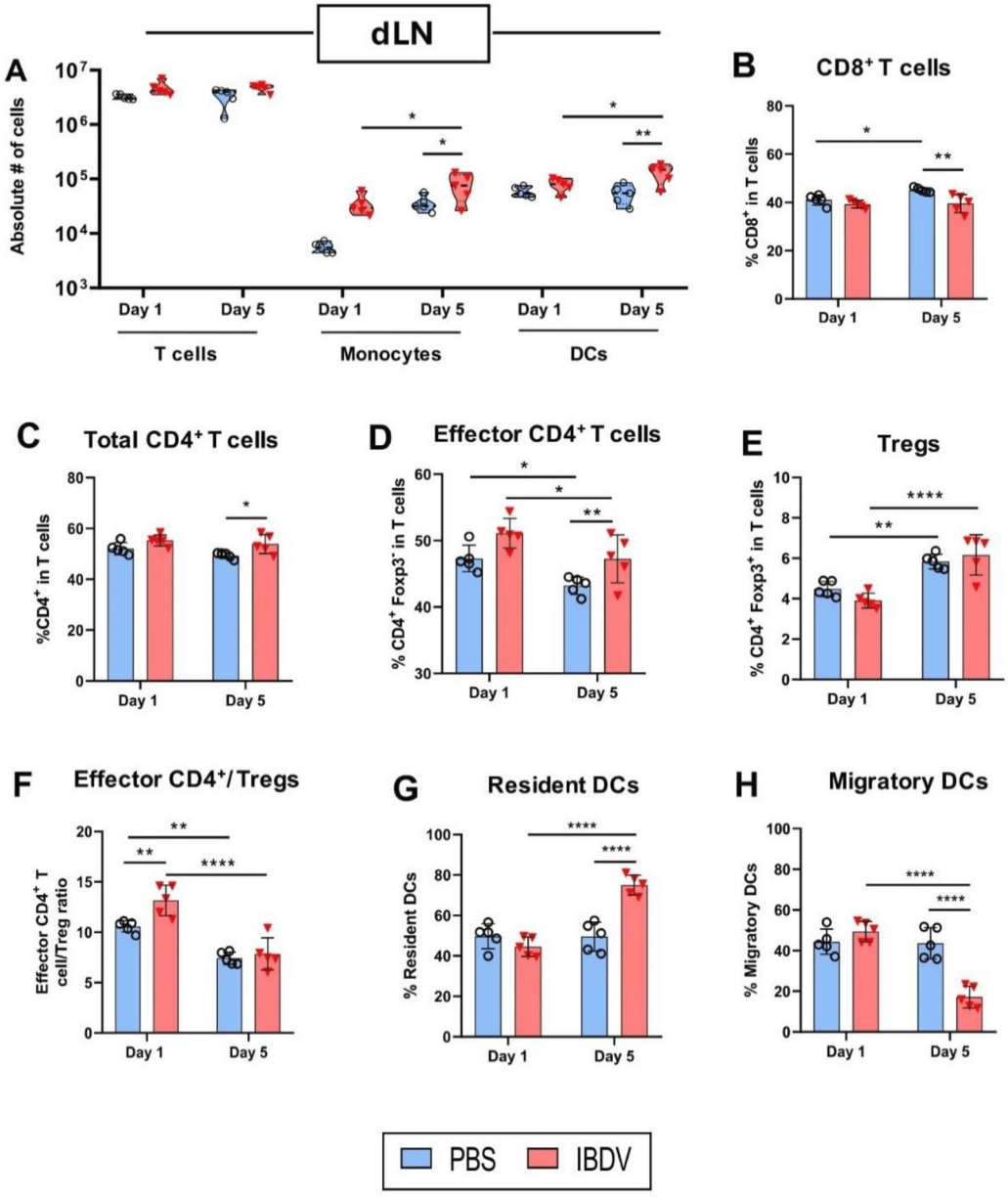

Figure 6 Immunophenotyping of tdLN in CT-2A murine GBM model. (A) Analysis of immune populations in tdLN: temporal distribution of immune cell populations within tdLN of IBDV/PBS-treated mice over the course of the treatment. (B–H) Analysis of myeloid and lymphoid immune cell populations in tdLN: changes in lymphoid and antigen-presenting cells were analyzed in IBDV-treated mice compared with PBS-treated mice in both groups (day 1 and 5). Two-way ANOVA analysis: *p<0.05; ***p<0.001; ****p<0.0001. ANOVA, analysis of variance; tdLN, tumor-lymph nodes; GBM, glioblastoma; IBDV, infectious bursal disease virus; PBS, phosphate-buffered saline; Treg, regulatory T cell.

MHC-II+) (figure 6I; online supplemental figure S5A-C). This effect was accompanied by an increased presence of inflammatory M1-like macrophages (CD11c−, CD11b+, Ly6G−, Ly6C+, MHC-II+) in mice treated with a single dose of IBDV (figure 5H).

Overall, IBDV virotherapy demonstrated significant impact on TME remodeling, reducing the presence of immunosuppressive populations and promoting T-cell functions.

IBDV therapy induces CD8+ T-cell migration and expansion of effector CD4+ T cells in tumor-draining lymph nodes

As tdLNs are pivotal hubs for initiating adaptive immune responses against tumors, their immune makeup was analyzed in the context of IBDV treatment by flow cytometry. Results presented no variation in the number of total T cells, but a higher infiltration of monocytes and DCs in the tdLN of mice treated with three injections of IBDV as compared with the PBS-treated control mice (figure 6A). Furthermore, the abundance of conventional type II DCs (cDC2) increased with repeated IBDV treatment (online supplemental figure 6D) denoting a sustained stimulation of DC migration.

T-cell analysis revealed a modest reduction in the percentage of cytotoxic CD8+T cells (figure 6B) accompanied by a significant increase in total CD4+T cells in IBDV-treated mice following three injections (figure 6C). The increase in total CD4+T cells was mainly due to effector helper T cells (figure 6D) rather than Tregs (figure 6E). Notably, the proportions of Tregs were already influenced by a higher ratio of effector CD4+T cells to Treg in mice treated with a single injection of IBDV (figure 6F). This suggests that, at this stage, helper T cells outnumbered compared with the immunosuppressive Tregs. Lastly, mice treated with three injections of IBDV showed an increase in resident DCs (intermediate major histocompatibility complex (MHC)-II) (figure 6G) while migratory DCs (high MHC-II) were significantly reduced (figure 6H) in tdLNs.

These findings highlight IBDV's capacity to reshape key immunological hubs characterized by increased resident DCs, increased effector CD4+T cell responses, and reduced immunosuppressive Tregs.

IBDV virotherapy converts immunosuppressive macrophages into immunoreactive effectors in murine and human tumors

GBMs are among the so-called immune desert tumors, characterized by minimal, if any, cytotoxic CD8+T cells, dominance of myeloid immunosuppressive populations and poor antigen presentation, with DCs often preserved in a dysfunctional state due to the lack of inflammatory signaling.[48] In GBMs, glioma-associated macrophages and microglia (GAMs) are central regulators of GBM TME. Presenting a phenotype skewed towards an M2-like immunosuppressive state, GAMs could represent up to 40–50% of the TME and conditionate tumor progression, invasion, angiogenesis, immunosuppression and resistance to therapy.[49] M2-like GAMs presence is associated with poor clinical outcome and shorter survival and many ongoing works to improve these outcomes are focused on shifting this restrictive phenotype into an immunoreactive pro-antitumoral one.[50]

Our analysis of the myeloid compartment in mice carrying CT-2A tumors showed a rapid inflammatory response characterized by a reduction in the presence of immunosuppressive M2-like TAMs (CD11c−, CD11b+, Ly6G−, Ly6C−, MHC-II+). This effect was accompanied by an increased presence of inflammatory M1-like TAMs (CD11c−, CD11b+, Ly6G−, Ly6C+, MHC-II+) after a single dose of IBDV (figure 5H,I; online supplemental figure 5A-C).

Due to the importance of these findings, we wanted to further investigate whether this early effect induced by IBDV can also be translated into human immune cells. To do so, we carried out a study of ex vivo exposure to IBDV of tissue explants generated from a human GBM-IDH wild-type tumor biopsy (supplementary **figure 7A**). A TMZ-only (1 mM) and a combination TMZ-IBDV conditions (1 mM /10^7 viral particles) were also included in the experimental set-up, aiming to identify possible synergetic effects and for comparative purposes. Due to the characteristics of the model and the aim of the study, experimental conditions were set-up to 72 hours of sustained exposure, to warranty tissue stability, and we focused the analysis on the myeloid populations—myeloid-derived monocytes (MDMs) and DCs—as shown in the gating (supplementary **figure 7B**).

Explants exposed to IBDV showed a significant reduction in immunosuppressive M2-like macrophages (HLA-DR+, CD64+, CD14+, CD11b+, arginase I high) accompanied by a marked increase in inflammatory M1-like macrophages (HLA-DR+, CD64+, CD14+, CD11b+, arginase I low) (supplementary **figure 7D**). Compared with other treatment modalities, IBDV induced the most significant shift in MDMs polarization. Further analysis of the M1-like MDMs population revealed an immunoreactive phenotype, as indicated by the expression of CD80, confirming the functional reprogramming (supplementary **figure 7E**).

IBDV-treated samples exhibited a higher prevalence of DCs at the time of the analysis (supplementary **figure 7F**). Notably, while the proportion of activated DCs—characterized by elevated expression of CD80 and HLA-DR high—was greater than in both TMZ and control groups. Interestingly, the combination of TMZ and IBDV further enhanced APC reprogramming, resulting in a larger proportion of activated DCs (supplementary **figure 7G**). Given the observed synergistic effect on cell viability, this phenotype might be associated with a more immunostimulatory mode of cancer cell death induced by the combined treatment.

Overall, these results demonstrate that IBDV effectively reprograms the myeloid compartment in GBM, both in murine and human model systems, promoting a shift toward an immunoreactive phenotype and enhancing dendritic cell activation. This last effect is further

amplified when combined with TMZ, suggesting a synergistic immunostimulatory response.

DISCUSSION

IBDV is introduced here as a potential oncolytic virotherapy candidate with attributes that address key challenges in GBM, including immune evasion and resistance to chemotherapy. As an alternative to current treatments, it shows promise in activating both innate and adaptive immune responses and serving as a complementary agent in combination therapies.

Efficient innate immune activation is essential for a successful adaptive antitumor response.[51] The data presented here show the induction of some key gene markers of innate immune activation programs following IBDV infection in human and murine GBM cells, as well as myeloid cells. A notable feature of IBDV infection is its moderate pro-inflammatory response compared with NDV, as observed in some GBM cell lines (figure 2A–C) and M1-like BMDMs (figure 2F). This characteristic could potentially minimize the risk of excessive inflammation in specific CNS tumor contexts, where excessive inflammation can damage neural tissues.[52]

IBDV infection can induce type III IFN-mediated immune responses, stimulating *IL28B* and *Mx1* expression in GBM27 cells, which lack the type I IFN gene cluster.[14] This presents an opportunity to explore the priming of type III IFN-mediated immune responses in the context of type I IFN-deficient tumor cells as well as to compare these responses with cells possessing both type I and type III IFN pathways. Identifying factors that could promote an improved adaptive immune response while minimizing excessive inflammation will aid in reducing immunosuppressive effects associated with immunotherapeutic strategies.[53]

While in vitro quantitative PCR analyses revealed differences in expression of key inflammatory genes between IBDV-infected and NDV-infected cells, these differences did not translate into significant therapeutic differences in vivo in the CT-2A GBM model (figure 4D). Both viruses showed comparable efficacy in controlling tumor growth and extending survival (figure 4,F). However, despite the observed improvement, all treated mice eventually reached the experimental endpoint and were terminated, highlighting the necessity for further refinement of IBDV's therapeutic strategy.

To gain a deeper understanding of the immune responses that made IBDV-treated mice outperform controls in restricting tumor growth, flow cytometry was used to analyze key immune populations in the TME and tdLN. In the TME, results revealed a reduction in immunosuppressive cells, including M2-like macrophages (figure 5I) and Tregs (figure 5E), and an increase in cytotoxic CD8+T cells (figure 5C) and M1-like macrophages (figure 5H), associated with a more favorable immune landscape to prime antitumor responses.[54]

The analysis of tdLN revealed additional insights into the immune dynamics induced by IBDV treatment. A marked increase in effector CD4+T cells (figure 6D) suggests an enhanced priming and activation within the lymph nodes.[55] Concurrently, there was a reduction in Tregs (figure 6E), indicative of a shift away from immunosuppressive conditions.[56 57] Notably, a lower presence of CD8+T cells in the tdLN (figure 6B) implies a potential migration of these cytotoxic cells toward the tumor, reinforcing the idea of a coordinated systemic immune response being directed against the GBM tumor.[58 59]

While these results demonstrate the robust immunostimulatory effect of intratumoral administration of IBDV, the treatment failed to elicit long-lasting responses that resolve in tumor elimination. For instance, the increase in migratory cDC2 rather than cDC1 suggests a priming of T cells that could lead to an antitumoral Th2 response or, alternatively, the priming of Tregs, counteracting an effective cytotoxic immune response by inducing immune tolerance (online supplemental figure S6).[60] Furthermore, while IBDV treatment induces a shift towards M1-like polarization in tumor macrophages (figure 5H), this does not translate into an activation of those macrophages, potentially limiting their contribution to the antitumoral immune response (online supplemental figure S5A). Similarly, while our results support an active T-cell engagement in response to IBDV, a deeper understanding of T-cell functionality could help to narrow down mechanisms of resistance due to T-cell exhaustion. Chronic inflammation within the TME can impair immune cell functionality.[61 62] Understanding how these immunological shifts contribute to tumor control and survival will be important to fully unlock IBDV potential as a virotherapeutic agent.

Early administration of IBDV and NDV treatments led to significant control of tumor growth and extended survival; however, complete tumor elimination was not observed, indicating the presence of resistance mechanisms that warrant further investigation. The inability to achieve sustained therapeutic responses, such as long-term survivors or complete responders, limited the scope of deeper analyses like tumor-specific and virus-specific T-cell profiling, which are essential for understanding the balance between antiviral and antitumor immune responses as well as the durability of IBDV-induced immunity. Nonetheless, this initial demonstration of the oncolytic and immunomodulatory potential of IBDV in GBM provides a solid foundation for future studies. The integration of translational strategies—optimized dosing, combinatorial regimens, and advanced responsive models—is anticipated to unlock conditions that enable comprehensive investigation of T-cell specificity and the mechanisms underpinning long-lasting antitumor immunity, advancing both mechanistic understanding and clinical application in the field of cancer virotherapy.

Our studies have demonstrated that IBDV can replicate and complement TMZ-induced cytotoxicity in vitro (figure 3; online supplemental figure S3). Moreover, exposure to TMZ did not impair GBMs' susceptibility to be infected by IBDV but potentiated the replication capacity and viral release of

the virus without diminishing antiviral responses. Furthermore, in our ex vivo GBM's explants study (supplementary figure 7), we detected a trend towards increased activation of APCs on the combination IBDV+TMZ treatment, as demonstrated by the percentage of $CD80^{+}$-HLA-DR (high) DCs, initially supporting the idea that the combination might be more immunogenic than the monotherapies. Yet, although our data provide insights into the multimodal advantage of pairing IBDV and TMZ, additional in vivo research is needed to explore the full scope and molecular basis of these findings to confirm the feasibility of this combination and support its clinical application.

In this regard, and based on similar observations, multiple studies aiming to overcome resistance to TMZ and to improve therapeutic outcomes have been focused on the combination of TMZ with different OVs:[63–65] the oncolytic adenovirus DNX-2401 has been tested alongside TMZ in patients with recurrent GBM (NCT01956734), showing enhanced survival benefits compared with monotherapy.[66] Similar synergistic effects have been observed in preclinical studies combining TMZ with oncolytic herpes simplex virus (G47Δ).[67 68] Chinese clinical trials have also used H101, an adenovirus-based OV, in combination with TMZ and chemoradiotherapy across various tumor types (ChiCTR2400085353). Overall, our data concurred with these advanced studies supporting that TMZ can enhance viral replication or immune activation, improving therapeutic outcomes.

In conclusion, IBDV presents an oncolytic profile that combines direct oncolysis, TME remodeling, and immune system activation. Its non-human origin further adds to its appeal, potentially enabling it to evade pre-existing immune responses that might limit the efficacy of other virotherapies.[69] These attributes make it a promising candidate for addressing unmet needs in GBM treatment. Further preclinical and clinical evaluations are essential to fully unlock its potential to expand its application in oncolytic virotherapy.

Author affiliations
[1]Department of Microbiology, Icahn School of Medicine at Mount Sinai, New York, New York, USA
[2]Microbiology Section, Departamento de Ciencias Farmacéuticas y de la Salud, Facultad de Farmacia, Universidad San Pablo-CEU, CEU Universities, Madrid, Spain
[3]Department of Basic Medical Sciences, Facultad de Medicina, Instituto de Medicina Molecular Aplicada-Nemesio Díez (IMMA-ND), Universidad San Pablo-CEU, CEU Universities, Institute of Applied Molecular Medicine (IMMA), Madrid, Spain
[4]Faculty of Experimental Sciences, Universidad Francisco de Vitoria, Pozuelo de Alarcón, Community of Madrid, Spain
[5]Department of Oncological Science, Icahn School of Medicine at Mount Sinai, New York, NY, USA
[6]National Center of Microbiology, Instituto de Salud Carlos III, Madrid, Community of Madrid, Spain
[7]Laboratorio de Inmunobiología de Trasplante e Inmunoterapia, Instituto de Biología Molecular (INBIOMIC), Universidad de León, León, Spain
[8]Global Health and Emerging Pathogens Institute, Icahn School of Medicine at Mount Sinai, New York, NY, USA
[9]Department of Medicine, Division of Infectious Diseases, Icahn School of Medicine at Mount Sinai, New York, NY, USA
[10]Department of Pathology, Molecular and Cell-Based Medicine, Icahn School of Medicine at Mount Sinai, New York, NY, USA
[11]The Tisch Cancer Institute, Icahn School of Medicine at Mount Sinai, New York, NY, USA
[12]The Icahn Genomics Institute, Icahn School of Medicine at Mount Sinai, New York, NY, USA
[13]Centro de Investigación en ciencias de la alimentación CSIC-UAM, CIAL, Madrid, Community of Madrid, Spain
[14]Faculty of Medicine, Universidad Francisco de Vitoria, Madrid, Spain
[15]Brain Tumour Laboratory, Fundación Vithas, Grupo Hospitales Vithas, Madrid, Spain
[16]Marc and Jennifer Lipschultz Precision Immunology Institute (PrIISM), Icahn School of Medicine at Mount Sinai, New York, NY, USA

Acknowledgements We would like to express our deepest gratitude to José F Rodríguez and Dolores Rodríguez for their support and guidance in Infectious Bursal Disease Virus (IBDV). We also sincerely thank Granja Rodríguez Serrano, located in Alba de Tormes, Salamanca, Spain, for generously providing chicken embryonated eggs for this research. The authors wish to express their deepest gratitude to the "Fundación Nemesio Diez" for its generous support and commitment to advancing meaningful and high-quality scientific research.

Contributors VT-P, SC-C: experimental design, methodology, investigation, analysis, writing, review and editing. YB, GD, LP-R, SI-L, SR-R, IP-A, JA-H, AM-S, IM-L: investigation and analysis. NG-R, DL-O: experimental design, methodology, review and editing. AG-S, JC-O, M-LdR, J-IR-B: methodology, review and editing. EN-V, AA-S: experimental design, review and editing. Guarantor: SC-C.

Funding This study has been funded by Instituto de Salud Carlos III (ISCIII) through the project "PI21/01353" and co-funded by the European Union.

Competing interests The AG-S laboratory has received research support from GSK, Pfizer, Senhwa Biosciences, Kenall Manufacturing, Blade Therapeutics, Avimex, Johnson & Johnson, Dynavax, 7Hills Pharma, Pharmamar, ImmunityBio, Accurius, Nanocomposix, Hexamer, N-fold LLC, Model Medicines, Atea Pharma, Applied Biological Laboratories and Merck. AG-S has consulting agreements for the following companies involving cash and/or stock: Castlevax, Amovir, Vivaldi Biosciences, Contrafect, 7Hills Pharma, Avimex, Pagoda, Accurius, Esperovax, Applied Biological Laboratories, Pharmamar, CureLab Oncology, CureLab Veterinary, Synairgen, Paratus, Pfizer, Virofend Therapeutics and Prosetta. AG-S has been an invited speaker in meeting events organized by Seqirus, Janssen, Abbott, AstraZeneca and Novavax. AG-S is an inventor on patents and patent applications on the use of antivirals and vaccines for the treatment and prevention of virus infections and cancer, owned by the Icahn School of Medicine at Mount Sinai, New York, USA, outside of the reported work. SC-C is the inventor on patents on the use of different viral platforms to treat cancer, owned by the Icahn School of Medicine at Mount Sinai, New York, USA. SC-C is co-founder of ViroFend Therapeutics SL.

Patient consent for publication Not applicable.

Ethics approval Not applicable.

Provenance and peer review Not commissioned; externally peer reviewed.

Data availability statement All data relevant to the study are included in the article or uploaded as supplementary information.

ORCID iDs
Jose-Ignacio Rodriguez-Barbosa https://orcid.org/0000-0001-7427-5654
Estanislao Nistal-Villan https://orcid.org/0000-0003-2458-8833
Sara Cuadrado-Castano https://orcid.org/0000-0002-9400-746X

REFERENCES

1 Gittleman H,QT, Farah P, Ondracek A, *et al*. CBTRUS statistical report: Primary brain and central nervous system tumors diagnosed in the United States in 2006-2010. *Neuro Oncol* 2013;15 Suppl 2.
2 Louis DN, Perry A, Wesseling P, *et al*. The 2021 WHO Classification of Tumors of the Central Nervous System: a summary. *Neuro-oncology* 2021;23:1231–51.
3 Stupp R, Mason WP, van den Bent MJ, *et al*. Radiotherapy plus concomitant and adjuvant temozolomide for glioblastoma. *N Engl J Med* 2005;352:987–96.
4 Lee SY. Temozolomide resistance in glioblastoma multiforme. *Genes & Diseases* 2016;3:198–210.
5 Zhan C, Lu W. The blood-brain/tumor barriers: challenges and chances for malignant gliomas targeted drug delivery. *Curr Pharm Biotechnol* 2012;13:2380–7.
6 DeCordova S, Shastri A, Tsolaki AG, *et al*. Molecular Heterogeneity and Immunosuppressive Microenvironment in Glioblastoma. *Front Immunol* 2020;11:1402.
7 Lathia JD, Mack SC, Mulkearns-Hubert EE, *et al*. Cancer stem cells in glioblastoma. *Genes Dev* 2015;29:1203–17.
8 Velásquez C, Mansouri S, Gutiérrez O, *et al*. Hypoxia Can Induce Migration of Glioblastoma Cells Through a Methylation-Dependent Control of *ODZ1* Gene Expression. *Front Oncol* 2019;9:1036.
9 Sundar SJ, Hsieh JK, Manjila S, *et al*. The role of cancer stem cells in glioblastoma. *Neurosurg Focus* 2014;37:E6.
10 Reis GF, Pekmezci M, Hansen HM, *et al*. CDKN2A loss is associated with shortened overall survival in lower-grade (World Health Organization Grades II-III) astrocytomas. *J Neuropathol Exp Neurol* 2015;74:442–52.
11 Ichimura K, Bolin MB, Goike HM, *et al*. Deregulation of the p14ARF/MDM2/p53 pathway is a prerequisite for human astrocytic gliomas with G1-S transition control gene abnormalities. *Cancer Res* 2000;60:417–24.
12 Dreyling MH, Bohlander SK, Adeyanju MO, *et al*. Detection of CDKN2 deletions in tumor cell lines and primary glioma by interphase fluorescence in situ hybridization. *Cancer Res* 1995;55:984–8.
13 Zhang H, Chen ZH, Savarese TM. Codeletion of the genes for p16INK4, methylthioadenosine phosphorylase, interferon-alpha1, interferon-beta1, and other 9p21 markers in human malignant cell lines. *Cancer Genet Cytogenet* 1996;86:22–8.
14 García-Romero N, Palacín-Aliana I, Esteban-Rubio S, *et al*. Newcastle Disease Virus (NDV) Oncolytic Activity in Human Glioma Tumors Is Dependent on CDKN2A-Type I IFN Gene Cluster Codeletion. *Cells* 2020;9:1405.
15 Harrington K, Freeman DJ, Kelly B, *et al*. Optimizing oncolytic virotherapy in cancer treatment. *Nat Rev Drug Discov* 2019;18:689–706.
16 Pikor LA, Bell JC, Diallo J-S. Oncolytic Viruses: Exploiting Cancer's Deal with the Devil. *Trends Cancer* 2015;1:266–77.
17 Lemos de Matos A, Franco LS, McFadden G. Oncolytic Viruses and the Immune System: The Dynamic Duo. *Molecular Therapy - Methods & Clinical Development* 2020;17:349–58.
18 Lichty BD, Breitbach CJ, Stojdl DF, *et al*. Going viral with cancer immunotherapy. *Nat Rev Cancer* 2014;14:559–67.
19 Rius-Rocabert S, García-Romero N, García A, *et al*. Oncolytic Virotherapy in Glioma Tumors. *Int J Mol Sci* 2020;21:7604.
20 Maruyama Y, Sakurai A, Noda S, *et al*. Regulatory Issues: PMDA – Review of Sakigake Designation Products: Oncolytic Virus Therapy with Delytact Injection (Teserpaturev) for Malignant Glioma. *Oncologist* 2023;28:664–70.
21 Askari FS, Mohebbi A, Ning J, *et al*. Editorial: Recent advances in oncolytic virus therapy for brain tumors. *Front Cell Infect Microbiol* 2023;13.
22 Hamad A, Yusubalieva GM, Baklaushev VP, *et al*. Recent Developments in Glioblastoma Therapy: Oncolytic Viruses and Emerging Future Strategies. *Viruses* 2023;15:547.
23 Ye C, Han X, Yu Z, *et al*. Infectious Bursal Disease Virus Activates c-Src To Promote α4β1 Integrin-Dependent Viral Entry by Modulating the Downstream Akt-RhoA GTPase-Actin Rearrangement Cascade. *J Virol* 2017;91:1891.
24 Lin T-W, Lo C-W, Lai S-Y, *et al*. Chicken Heat Shock Protein 90 Is a Component of the Putative Cellular Receptor Complex of Infectious Bursal Disease Virus. *J Virol* 2007;81:8730–41.
25 Shah AU, Li Y, Ouyang W, *et al*. From nasal to basal: single-cell sequencing of the bursa of Fabricius highlights the IBDV infection mechanism in chickens. *Cell Biosci* 2021;11:212.
26 Jackwood DJ, Henderson KS, Jackwood RJ. Enzyme-linked immunosorbent assay-based detection of antibodies to antigenic subtypes of infectious bursal disease viruses of chickens. *Clin Diagn Lab Immunol* 1996;3:456–63.
27 Rekha K, Sivasubramanian C, Chung I-M, *et al*. Growth and replication of infectious bursal disease virus in the DF-1 cell line and chicken embryo fibroblasts. *Biomed Res Int* 2014;2014:494835.
28 Soleimani S,S, Mahravani H, Ebrahimi MM, *et al*. Mouse Fibroblast L929 Cell Line as a Useful Tool for Replication and Adaptation of Infectious Bursal Disease Virus. *Arch Razi Inst* 2023;78:863–71.
29 Jackwood DH, Saif YM, Hughes JH. Replication of infectious bursal disease virus in continuous cell lines. *Avian Dis* 1987;31:370–5.
30 Delgui LR, Rodríguez JF, Colombo MI. The endosomal pathway and the Golgi complex are involved in the infectious bursal disease virus life cycle. *J Virol* 2013;87:8993–9007.
31 Schirrmacher V. Molecular Mechanisms of Anti-Neoplastic and Immune Stimulatory Properties of Oncolytic Newcastle Disease Virus. *Biomedicines* 2022;10:562.
32 Bykov Y, Dawodu G, Javaheri A, *et al*. Immune responses elicited by ssRNA(-) oncolytic viruses in the host and in the tumor microenvironment. *J Cancer Metastasis Treat* 2023;9:10.
33 Wu Y-Y, Wu F-H, Chen I-C, *et al*. Oncolytic avian reovirus-sensitized tumor infiltrating CD8+ T cells triggering immunogenic apoptosis in gastric cancer. *Cell Commun Signal* 2024;22:514.
34 Javaheri A, Bykov Y, Mena I, *et al*. Avian Paramyxovirus 4 Antitumor Activity Leads to Complete Remissions and Long-term Protective Memory in Preclinical Melanoma and Colon Carcinoma Models. *Cancer Res Commun* 2022;2:602–15.
35 Kasloff SB, Pizzuto MS, Silic-Benussi M, *et al*. Oncolytic activity of avian influenza virus in human pancreatic ductal adenocarcinoma cell lines. *J Virol* 2014;88:9321–34.
36 Chumakov K. T. A Harmless Avian Vaccine Virus Could Be Developed into an Off-the-Shelf "Antibiotic" for Viruses. *Qeios* 2024.
37 Dalton RM, Rodríguez JF. Rescue of infectious birnavirus from recombinant ribonucleoprotein complexes. *PLoS ONE* 2014;9:e87790.
38 Reed LJ, Muench H. A simple method of estimating fifty per cent endpoints12. *Am J Epidemiol* 1938;27:493–7.
39 Livak KJ, Schmittgen TD. Analysis of Relative Gene Expression Data Using Real-Time Quantitative PCR and the 2−ΔΔCT Method. *Methods* 2001;25:402–8.
40 Cubas-Gaona LL, Diaz-Beneitez E, Ciscar M, *et al*. Exacerbated Apoptosis of Cells Infected with Infectious Bursal Disease Virus upon Exposure to Interferon Alpha. *J Virol* 2018;92.
41 Bai Y, Chen Y, Hong X, *et al*. Newcastle disease virus enhances the growth-inhibiting and proapoptotic effects of temozolomide on glioblastoma cells in vitro and in vivo. *Sci Rep* 2018;8:11470.
42 Dawodu G,Y, Javaheri A, Garcia-Sastre A, *et al*. Immune responses elicited by ssRNA(-) oncolytic viruses in the host and in the tumor microenvironment. *J Cancer Metastasis Treat* 2023;9:10.
43 Tur-Planells V, García-Sastre A, Cuadrado-Castano S, *et al*. Engineering Non-Human RNA Viruses for Cancer Therapy. *Vaccines (Basel)* 2023;11:1617.
44 Khatri M, Sharma JM. Modulation of macrophages by infectious bursal disease virus. *Cytogenet Genome Res* 2007;117:388–93.
45 Khan F, Pang L, Dunterman M, *et al*. Macrophages and microglia in glioblastoma: heterogeneity, plasticity, and therapy. *J Clin Invest* 2023;133.
46 Kotecha R, Odia Y, Khosla AA, *et al*. Key Clinical Principles in the Management of Glioblastoma. *JCO Oncol Pract* 2023;19:180–9.
47 Serrano-Chávez E, Halldórsdóttir HR, Engel TB, *et al*. An in situ depot for the sustained release of a TLR7/8 agonist in combination with a TGFβ inhibitor promotes anti-tumor immune responses. *Nat Commun* 2024;15:7687.
48 Wang G, Zhong K, Wang Z, *et al*. Tumor-associated microglia and macrophages in glioblastoma: From basic insights to therapeutic opportunities. *Front Immunol* 2022;13:964898.
49 Xuan W, Lesniak MS, James CD, *et al*. Context-Dependent Glioblastoma-Macrophage/Microglia Symbiosis and Associated Mechanisms. *Trends Immunol* 2021;42:280–92.
50 Montemurro N, Pahwa B, Tayal A, *et al*. Macrophages in Recurrent Glioblastoma as a Prognostic Factor in the Synergistic System of the Tumor Microenvironment. *Neurol Int* 2023;15:595–608.
51 Li W, Zhang Q, Li Q, *et al*. n.d. Innate immune response restarts adaptive immune response in tumors. *Front Immunol*14.
52 Dahm T, Rudolph H, Schwerk C, *et al*. Neuroinvasion and Inflammation in Viral Central Nervous System Infections. *Mediators Inflamm* 2016;2016:1–16.
53 Reversing immunosenescence with senolytics to enhance tumor immunotherapy. 2024.
54 Noorani I, Sidlauskas K, Pellow S, *et al*. Clinical impact of anti-inflammatory microglia and macrophage phenotypes at glioblastoma margins. *Brain Communications* 2023;5:fcad176.
55 Khan SM, Desai R, Coxon A, *et al*. Impact of CD4 T cells on intratumoral CD8 T-cell exhaustion and responsiveness to PD-1

blockade therapy in mouse brain tumors. *J Immunother Cancer* 2022;10:e005293.
56 Heimberger AB, Abou-Ghazal M, Reina-Ortiz C, *et al*. Incidence and Prognostic Impact of FoxP3+ Regulatory T Cells in Human Gliomas. *Clin Cancer Res* 2008;14:5166–72.
57 Wainwright DA, Balyasnikova IV, Chang AL, *et al*. IDO Expression in Brain Tumors Increases the Recruitment of Regulatory T Cells and Negatively Impacts Survival. *Clin Cancer Res* 2012;18:6110–21.
58 High endothelial venules control the journey of stem-like cd8+t cells from lymph node to tumor during cancer immunotherapy with combined anti-pd-1 plus anti-ctla-4 antibodies507 high endothelial venules control the journey of stem-like cd8+t cells from lymph node to tumor during cancer immunotherapy with combined anti-pd-1 plus anti-ctla-4 antibodies. 2022.
59 Wang AZ, Mashimo BL, Schaettler MO, *et al*. Glioblastoma-Infiltrating CD8+ T Cells Are Predominantly a Clonally Expanded GZMK+ Effector Population. *Cancer Discov* 2024;14:1106–31.
60 Saito Y, Komori S, Kotani T, *et al*. The Role of Type-2 Conventional Dendritic Cells in the Regulation of Tumor Immunity. *Cancers (Basel)* 2022;14:1976.
61 Fu Z, Xu H, Yue L, *et al*. Immunosenescence and cancer: Opportunities and challenges. *Medicine (Baltimore)* 2023;102:e36045.
62 Fornara O, Odeberg J, Wolmer Solberg N, *et al*. Poor survival in glioblastoma patients is associated with early signs of immunosenescence in the CD4 T-cell compartment after surgery. *Oncoimmunology* 2015;4:e1036211.
63 Kriuchkovskaia VA, Eames EK, Riggins RB, *et al*. Acquired Temozolomide Resistance Instructs Patterns of Glioblastoma Behavior in Gelatin Hydrogels. *Adv Healthc Mater* 2024;13:e2400779.
64 Bernstock JD, Blitz SE, Hoffman SE, *et al*. Recent oncolytic virotherapy clinical trials outline a roadmap for the treatment of high-grade glioma. *Neurooncol Adv* 2023;5:vdad081.
65 Zhou Y, Shi F, Zhu J, *et al*. An update on the clinical trial research of immunotherapy for glioblastoma. *Front Immunol* 2025;16.
66 Gallego Perez-Larraya J, García-Moure M, González-Huárriz M, *et al*. P17.14.B phase i trial of dnx-2401 oncolytic adenovirus combined with a short course of dose-dense temozolomide for recurrent glioblastoma. *Neuro-oncology* 2023;25:ii120.
67 Erickson NJ, Stavarache M, Tekedereli I, *et al*. Herpes Simplex Oncolytic Viral Therapy for Malignant Glioma and Mechanisms of Delivery. *World Neurosurg* 2025;194:123595.
68 Todo T, Ito H, Ino Y, *et al*. Intratumoral oncolytic herpes virus G47Δ for residual or recurrent glioblastoma: a phase 2 trial. *Nat Med* 2022;28:1630–9.
69 Groeneveldt C, van den Ende J, van Montfoort N. Preexisting immunity: Barrier or bridge to effective oncolytic virus therapy? *Cytokine Growth Factor Rev* 2023;70:1–12.